

Matrix Infrared Spectra and Density Functional Calculations of $\text{Co}(\text{CO})_x^-$ ($x = 1, 2, 3, 4$) Anions

Mingfei Zhou and Lester Andrews*

Department of Chemistry, University of Virginia, Charlottesville, Virginia 22901

Received: July 28, 1998; In Final Form: October 19, 1998

Laser-ablated cobalt atoms have been reacted with CO molecules during condensation in excess argon. The CoCO molecule is observed after deposition, and $\text{Co}(\text{CO})_{2,3,4}$ are formed on annealing in agreement with earlier matrix work. Cobalt carbonyl anions are also produced and trapped. On the basis of isotopic substitution and density functional calculations, a sharp absorption at 1804.0 cm^{-1} is assigned to the C–O stretching mode of CoCO^- , 1768.9 and 1860.2 cm^{-1} bands to antisymmetric and symmetric C–O stretching vibrations of bent $\text{Co}(\text{CO})_2^-$, and 1826.9 and 1890.0 cm^{-1} absorptions to the antisymmetric stretching modes of $\text{Co}(\text{CO})_3^-$ and $\text{Co}(\text{CO})_4^-$, respectively.

Introduction

Cobalt carbonyls and complexes are important in processes such as organometallic synthesis and homogeneous catalysis.¹ Neutral cobalt carbonyls have been well studied both by experiment^{2–6} and theory.^{7–10} First $\text{Co}(\text{CO})_4$ was produced by pyrolysis of $\text{Co}_2(\text{CO})_8$ and photolysis of $\text{Co}(\text{CO})_3(\text{NO})$.^{2–5} The cobalt carbonyls $\text{Co}(\text{CO})_{1–4}$ were formed via thermal Co atom reactions with CO molecules and characterized by matrix IR and ESR spectroscopy.⁶ Finally, $\text{Co}(\text{CO})_4$ has been studied by early extended Huckel type calculations,^{9,10} and density functional calculations of $\text{Co}(\text{CO})_{1–4}$ have been reported.⁸

Compared to the neutral carbonyls, little work has been done on carbonyl anions. Only $\text{Co}(\text{CO})_4^-$ has been observed in THF solution,¹¹ and calculations suggest that $\text{Co}(\text{CO})_4^-$ is tetrahedral and $\text{Co}(\text{CO})_3^-$ is planar or near planar.¹⁰ The bond strengths in $\text{Co}(\text{CO})_4^-$ and $\text{Co}(\text{CO})_3^-$ have been determined from collisional induced dissociation investigations.¹²

Recent pulsed laser-ablation matrix isolation studies on the Fe and Ni + CO systems^{13,14} have shown that, in contrast to thermal atom sources, electrons are produced in the laser-ablation process, and anions can be formed via electron capture by neutral molecules during matrix condensation. In this paper, we report the reaction of laser-ablated cobalt atoms and electrons with CO molecules during condensation in excess argon. Besides the neutral $\text{Co}(\text{CO})_x$ molecules, the $\text{Co}(\text{CO})_x^-$ ($x = 1, 2, 3, 4$) anions are also produced and trapped in the matrix and identified by isotopic substitution and density functional calculations.

Experimental Section

The experiment for laser ablation and matrix isolation has been described in detail previously.¹⁵ Briefly, the Nd:YAG laser fundamental (1064 nm, 10 Hz repetition rate with 10 ns pulse width) was focused on the rotating cobalt metal target (Johnson Matthey, 99.9%). Laser-ablated metal atoms were co-deposited with carbon monoxide (0.4%) in excess argon onto a 10 K CsI cryogenic window at 2–4 mmol/h for 1–2 h. Carbon monoxide (Matheson) and isotopic precursors $^{13}\text{C}^{16}\text{O}$ and $^{12}\text{C}^{18}\text{O}$ (Cambridge Isotopic Laboratories) and $^{12}\text{C}^{16}\text{O} + ^{13}\text{C}^{16}\text{O}$, $^{12}\text{C}^{16}\text{O} + ^{12}\text{C}^{18}\text{O}$ mixtures were used in different experiments. FTIR spectra were recorded at 0.5 cm^{-1} resolution on a Nicolet 750

spectrometer with 0.1 cm^{-1} accuracy using a HgCdTe detector. Matrix samples were annealed at different temperatures and subjected to different wavelength photolysis using a tungsten lamp (Sylvania, DEK, 500 W) or a medium-pressure mercury arc (Philips, H39KB, 175 W) lamp and glass filters.

Results

Matrix infrared spectra and density functional calculations on cobalt carbonyl molecules and anions will be presented.

Infrared Spectra. The infrared spectra of laser-ablated cobalt atoms co-deposited with 0.4% CO in argon are shown in Figures 1 and 2, and the absorptions are listed in Table 1. The spectrum in the 2080–1910 cm^{-1} region is very similar to that from thermal atom reactions reported by the Ozin group.⁶ Product absorptions were observed at 1960.7 and 1957.3 cm^{-1} after deposition; annealing to 20 K produced bands at 1920.8 and 1983.2 cm^{-1} , and another annealing to 25 K increased these two bands and produced extra bands at 2016.6, 2023.5 cm^{-1} , 2045.5, 2053.0 cm^{-1} , and 2062.4 cm^{-1} .

Figure 2 shows spectra in the 1900–1760 cm^{-1} region, which are of particular interest here. Sharp new bands at 1804.0, 1809.3 cm^{-1} and weak bands at 1768.9, 1860.2 cm^{-1} were observed after deposition. Annealing to 20 K decreased the 1804.0 cm^{-1} band and increased the 1809.3 cm^{-1} absorption, whereas 25 K annealing decreased both bands and increased the 1768.9, 1860.2 cm^{-1} bands and produced new bands at 1826.9 and 1890.0 cm^{-1} . Filtered infrared photolysis (630–1000 nm) with a 500 W tungsten lamp reduced the 1804.0 and 1809.3 cm^{-1} bands about 50%, with no effect on the other bands. This lamp output in the 470–1000 nm region totally destroyed the 1804.0 and 1809.3 cm^{-1} bands, reduced the 1826.9 cm^{-1} band about 50%, and produced a new band at 1820.0 cm^{-1} . Mercury arc photolysis with a 380 nm long-wavelength pass filter destroyed the 1768.9 and 1860.2 cm^{-1} bands, with no change in the 1820.0, 1826.9, and 1890.0 cm^{-1} bands. Another photolysis using a 290 nm long-wavelength pass filter decreased the 1820.0 and 1826.9 cm^{-1} bands about 50% and slightly increased the 1890.0 cm^{-1} band. Final full arc photolysis destroyed the 1820.0, 1826.9, and 1890.0 cm^{-1} bands. None of these bands came back on further annealing to 30 and 35 K. In addition, weaker bands at 547.7, 525.7, 484.9, and 463.3 cm^{-1} appeared on annealing.

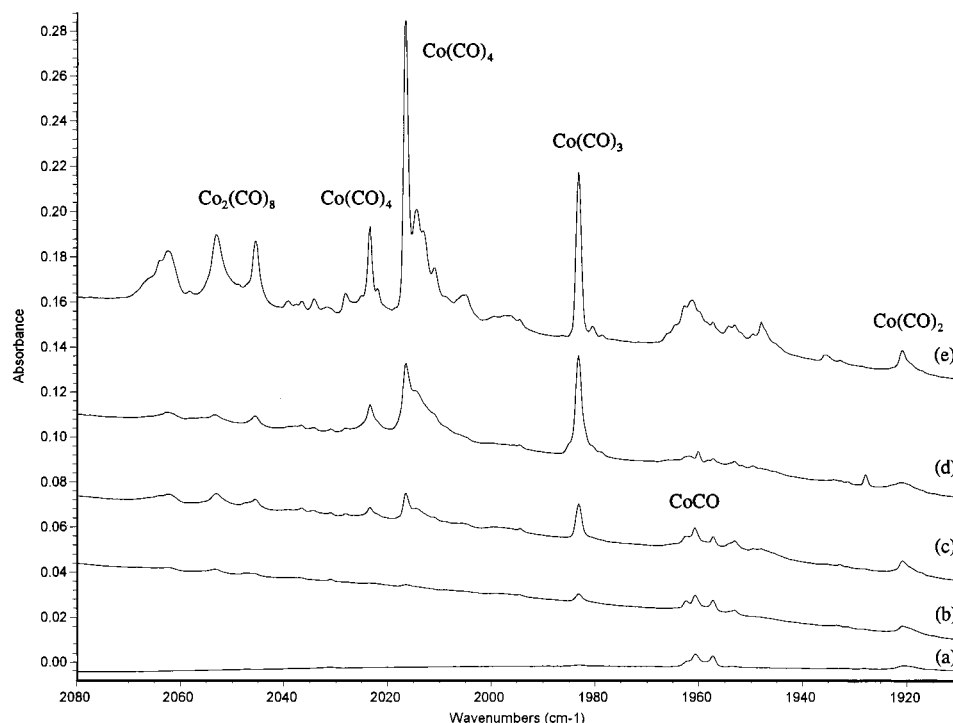


Figure 1. Infrared spectra in the 2080–1910 cm^{-1} region for laser-ablated cobalt atoms co-deposited with 0.4% CO in excess argon: (a) after 1.5 h sample deposition at 10 K, (b) after annealing to 20 K, (c) after annealing to 25 K, (d) after 10 min full Hg arc photolysis, and (e) after annealing to 30 K.

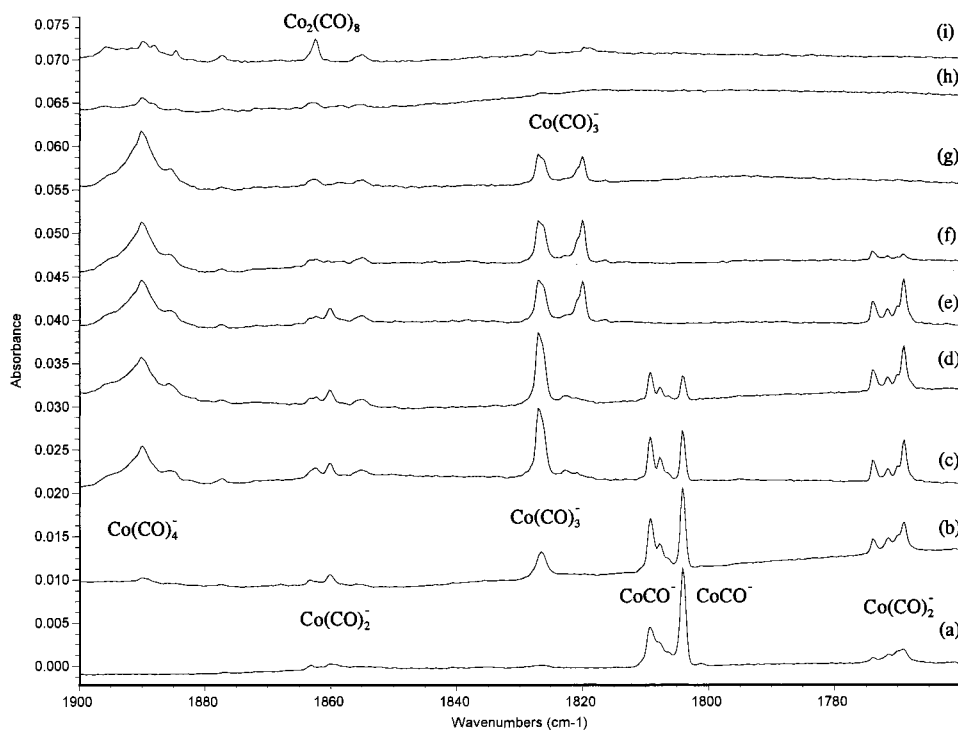


Figure 2. Infrared spectra in the 1900–1760 cm^{-1} region for laser-ablated cobalt atoms co-deposited with 0.4% CO in argon: (a) after 1.5 h sample deposition at 10 K, (b) after annealing to 20 K, (c) after annealing to 25 K, (d) after 10 min 630–1000 nm W-lamp photolysis, (e) after 10 min W-lamp 470–1000 nm photolysis, (f) after 10 min >380 nm Hg-arc photolysis, (g) after 10 min >290 nm Hg-arc photolysis, (h) after 10 min full Hg-arc photolysis, and (i) after annealing to 30 K.

A sharp 1515.5 cm^{-1} band observed after deposition (not shown in figure) is due to $(\text{CO})_2^-$.^{13,14,16} This band and its isotopic counterparts decreased slightly on annealing, decreased 50% on 380–1000 nm photolysis, and disappeared on 290–1000 nm photolysis.

Isotopic substitution was employed for characterization of absorptions. Similar spectra were observed using $^{13}\text{C}^{16}\text{O}$ and $^{12}\text{C}^{18}\text{O}$ samples, and the results were also listed in Table 1.

Experiments with mixed $^{12}\text{C}^{16}\text{O} + ^{13}\text{C}^{16}\text{O}$ and $^{12}\text{C}^{16}\text{O} + ^{12}\text{C}^{18}\text{O}$ isotopic precursors were also done, and spectra in the 1900–1720 cm^{-1} region are shown in Figures 3 and 4 and in the 2070–1870 cm^{-1} region in Figures 5 and 6. Doublets were observed for the 1804.0, 1809.3, 1957.3, and 1960.7 cm^{-1} absorptions, triplets were observed for the 1768.9, 1860.2, and 1920.8 cm^{-1} absorptions, and quartets for the 1820.0, 1826.9, and 1983.2 cm^{-1} bands in both mixed isotopic experiments.

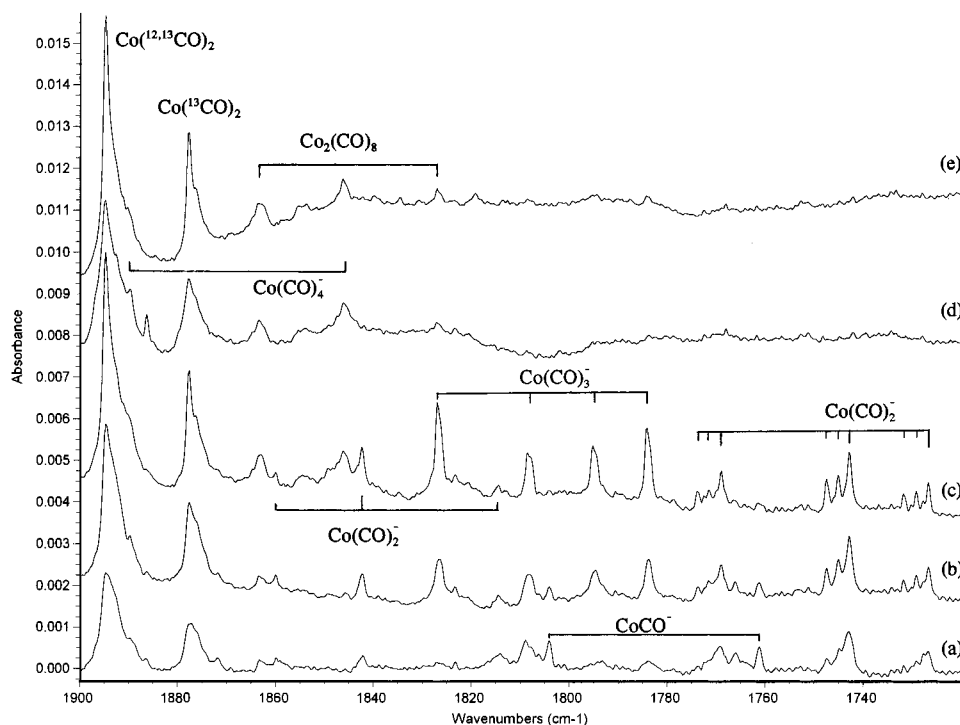


Figure 3. Infrared spectra in the 1900–1720 cm^{-1} region for laser-ablated cobalt atoms co-deposited with 0.2% $^{12}\text{C}^{16}\text{O}$ + 0.2% $^{13}\text{C}^{16}\text{O}$ in argon: (a) after 1.5 h sample deposition at 10 K, (b) after annealing to 20 K, (c) after annealing to 25 K, (d) after 10 min >380 nm Hg-arc photolysis, and (e) after annealing to 30 K.

TABLE 1: Infrared Absorptions (cm^{-1}) from Co-Deposition of Laser-Ablated Cobalt Atoms with Carbon Monoxide in Excess Argon at 10 K

$^{12}\text{C}^{16}\text{O}$	$^{13}\text{C}^{16}\text{O}$	$^{12}\text{C}^{18}\text{O}$	$^{12}\text{C}^{16}\text{O} + ^{13}\text{C}^{16}\text{O}$	$^{12}\text{C}^{16}\text{O} + ^{12}\text{C}^{18}\text{O}$	$R(12/13)$	$R(16/18)$	assignment
2138.1	2091.1	2087.1			1.022 48	1.024 44	CO
2062.4	2016.9	2014.2			1.022 56	1.023 93	$\text{Co}_x(\text{CO})_y$
2053.0	2005.7	2007.1			1.023 58	1.022 87	$\text{Co}_2(\text{CO})_8$
2045.5	1999.1	1999.8			1.023 21	1.022 85	$\text{Co}_2(\text{CO})_8$
2028.2	1982.4	1982.3			1.023 10	1.023 15	$\text{Co}_2(\text{CO})_8$
2023.5	1977.9	1977.2			1.023 05	1.023 42	$\text{Co}(\text{CO})_4$
2016.6	1971.4	1970.0			1.022 93	1.023 65	$\text{Co}(\text{CO})_4$
2014.4	1969.4	1967.9			1.022 85	1.023 63	$\text{Co}(\text{CO})_4$ site
1983.2	1938.8	1937.5	1983.2, 1963.3, 1949.8, 1938.8	1983.2, 1963.2, 1949.1, 1937.4	1.022 90	1.023 59	$\text{Co}(\text{CO})_3$
1960.7	1913.5	1920.6	1960.6, 1913.4	1960.7, 1920.5	1.024 67	1.020 88	CoCO site
1957.3	1910.1	1917.2	1957.2, 1910.2	1957.2, 1917.2	1.024 71	1.020 92	CoCO
1953.2	1908.4	1909.7			1.023 48	1.022 78	$\text{Co}_x(\text{CO})_y$
1948.0	1904.4	1903.2			1.022 89	1.023 54	$\text{Co}_x(\text{CO})_y$
1927.9	1886.4	1881.2	1928.0, 1903.8, 1886.4	1928.0, 1901.4, 1881.2	1.022 00	1.024 82	$\text{Co}(\text{CO})_2$ site
1920.8	1877.8	1877.0	1920.9, 1894.7, 1788.7	1920.7, 1894.9, 1876.9	1.022 90	1.023 34	$\text{Co}(\text{CO})_2$
1890.0	1846.3	1849.0			1.023 67	1.022 17	$\text{Co}(\text{CO})_4^-$
1862.4	1819.8	1821.0			1.023 41	1.022 73	$\text{Co}_2(\text{CO})_8$
1860.2	1814.5	1823.2	1860.2, 1842.5, 1814.5	1860.2, 1845.1, 1823.2	1.025 19	1.020 29	$\text{Co}(\text{CO})_2^-$
1826.9	1784.2	1787.6	1826.9, 1808.6, 1795.2, 1784.2	1826.8, 1810.6, 1798.0, 1787.5	1.023 93	1.021 98	$\text{Co}(\text{CO})_3^-$
1820.0	1777.7	1780.5		1820.1, 1804.1, 1791.3, 1780.5	1.023 79	1.022 18	$\text{Co}(\text{CO})_3^-$ site
1809.2	1766.2	1771.5			1.024 35	1.021 28	CoCO ⁻ site
1807.7	1764.7	1770.2			1.024 37	1.021 18	CoCO ⁻ site
1804.0	1761.0	1766.8	1804.1, 1761.2	1804.2, 1767.0	1.024 42	1.021 06	CoCO ⁻
1773.9	1731.8	1736.7	1773.9, 1747.5, 1731.8	1773.9, 1751.5, 1736.5	1.024 31	1.021 42	$\text{Co}(\text{CO})_2^-$ site
1771.5	1729.2	1735.0	1771.6, 1745.1, 1729.2	1771.5, 1749.5, 1734.8	1.024 46	1.021 04	$\text{Co}(\text{CO})_2^-$ site
1768.9	1726.7	1732.5	1769.0, 1742.8, 1726.7	1769.0, 1747.3, 1732.6	1.024 44	1.021 01	$\text{Co}(\text{CO})_2^-$
1515.5	1482.2	1479.5	1515.5, 1497.4, 1482.2	1515.5, 1497.4, 1479.5	1.022 47	1.024 33	$(\text{CO})_2^-$
547.7	536.4	544.2			1.021 07	1.006 43	$\text{Co}_x(\text{CO})_y$
525.7	516.6				1.017 62		$\text{Co}_x(\text{CO})_y$
484.9		481.6				1.006 85	$\text{Co}(\text{CO})_4$?
463.3	458.3	454.8			1.010 91	1.018 69	$\text{Co}(\text{CO})_3$

Strong pure isotopic features were observed for the 2023.5 and 2016.6 cm^{-1} bands with several weaker intermediate components (see Figure 6d).

Another experiment was done with 0.5% CO and 0.05% CCl_4 added to serve as an electron trap. The product bands in the 2070–1900 cm^{-1} region were observed as before, but the new

product bands in the 1900–1720 cm^{-1} region were not observed with CCl_4 present.

Calculations. Density functional theory (DFT) calculations were performed using the Gaussian 94 program.¹⁷ The BP86 functional,¹⁸ 6-311+G* basis sets for carbon and oxygen,¹⁹ and the set of Wachters and Hay for cobalt²⁰ were used. Earlier pure

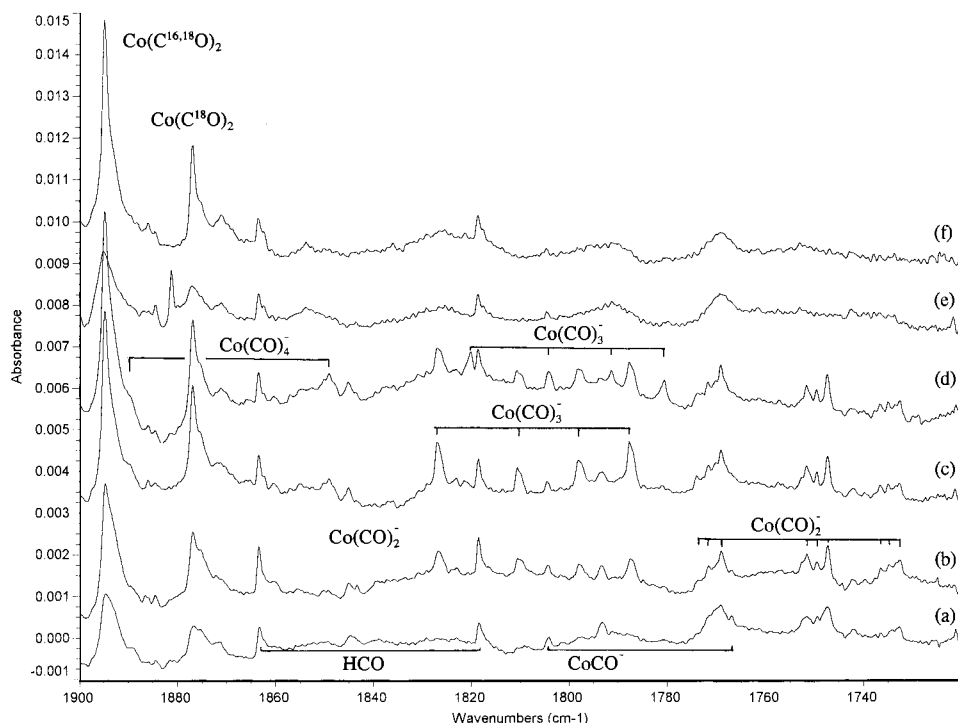


Figure 4. Infrared spectra in the $1900\text{--}1720\text{ cm}^{-1}$ region for laser-ablated cobalt atoms co-deposited with $0.2\% \text{ }^{12}\text{C}^{16}\text{O} + 0.2\% \text{ }^{12}\text{C}^{18}\text{O}$ in argon: (a) after 1.5 h sample deposition at 10 K, (b) after annealing to 20 K, (c) after annealing to 25 K, (d) after 10 min 470–1000 nm Hg-arc photolysis, (e) after 10 min full Hg-arc photolysis, and (f) after annealing to 30 K.

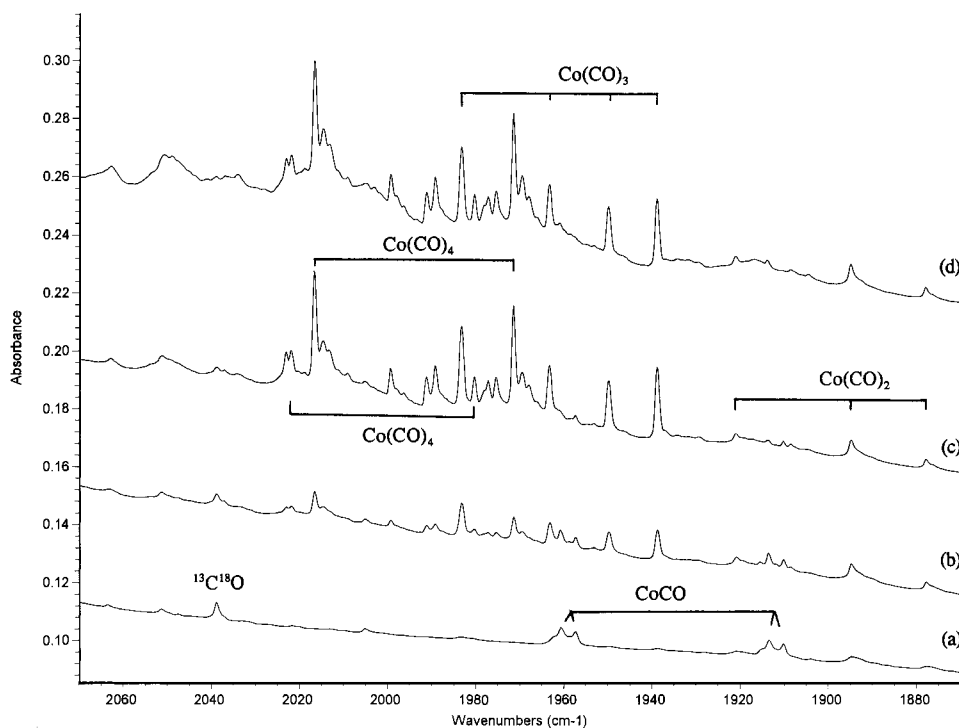


Figure 5. Infrared spectra in the $2070\text{--}1870\text{ cm}^{-1}$ region for laser-ablated cobalt atoms co-deposited with $0.2\% \text{ }^{12}\text{C}^{16}\text{O} + 0.2\% \text{ }^{13}\text{C}^{16}\text{O}$ in argon: (a) after 1.5 h sample deposition at 10 K, (b) after annealing to 20 K, (c) after annealing to 25 K, (d) after 10 min $>380\text{ nm}$ Hg-arc photolysis, and (e) after annealing to 30 K.

DFT calculations on CoCO by Fournier found the ${}^2\Delta$ state 16.7 kcal/mol lower than the ${}^4\Delta$ state and a 2052 cm^{-1} harmonic C–O stretching frequency.^{7a} Recently, Ryeng et al. reported DFT calculations for $\text{Co}(\text{CO})_{1-4}$ with the BP86 functional and Slater type orbital valence basis sets using the ADF program.⁸ All four carbonyls have doublet ground states. For comparison, the $\text{Co}(\text{CO})_{1-3}$ molecules were calculated here, and the very similar results are listed in Table 2. The monocarbonyl CoCO

is calculated to be a linear, ${}^2\Delta$ state with the same C–O bond length and C–O stretching frequency (1980.5 cm^{-1}), but Co–C bond length (1.682 \AA) slightly longer than the 1.667 \AA value calculated by the Swang group. Recent hybrid DFT calculations using the B3LYP functional gave a higher 2020 cm^{-1} frequency.^{7b} Since the present calculations are done to predict isotopic frequencies for comparison with experiment and the BP86 functional produces calculated frequencies in much better

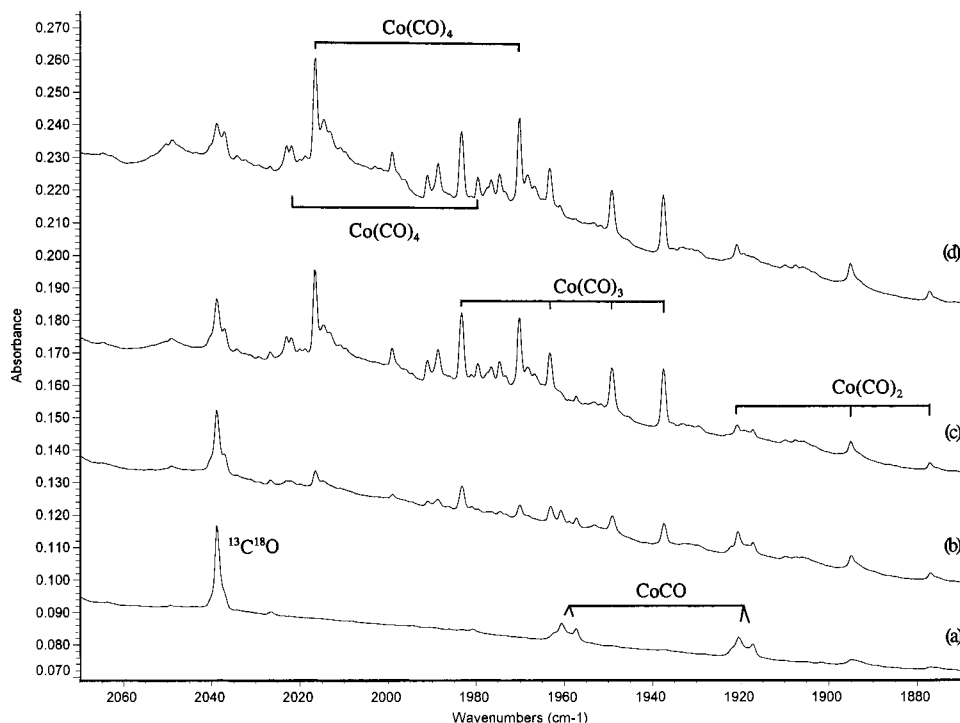


Figure 6. Infrared spectra in the 2070–1870 cm^{-1} region for laser-ablated cobalt atoms co-deposited with 0.2% $^{12}\text{C}^{16}\text{O}$ + 0.2% $^{12}\text{C}^{18}\text{O}$ in argon: (a) after 1.5 h sample deposition at 10 K, (b) after annealing to 20 K, (c) after annealing to 25 K, (d) after 10 min 470–1000 nm Hg-arc photolysis, (e) after 10 min full Hg-arc photolysis, and (f) after annealing to 30 K.

TABLE 2: Calculated (BP86/6-311+G*) Geometry, Isotopic C–O Stretching Frequencies (cm^{-1}), Intensities (km/mol), and Isotopic Frequency Ratios for $\text{Co}(\text{CO})_x$ ($x = 1, 2, 3$) Molecules

molecule	geometry	$^{12}\text{C}^{16}\text{O}$	$^{13}\text{C}^{16}\text{O}$	$^{12}\text{C}^{18}\text{O}$	$R(12/13)$	$R(16/18)$
$\text{CoCO } ^2\Delta$	Co–C, 1.682 Å; C–O, 1.17 Å; linear	1980.5(697)	1931.8(660)	1939.8(674)	1.025 21	1.020 98
$\text{Co}(\text{CO})_2 ^2A_1$	Co–C, 1.799 Å; C–O, 1.156 Å;	1972.8(2198)	1927.9(2066)	1926.6(2146)	1.023 29	1.023 98
	$\angle\text{CCoC}$, 171.9°; $\angle\text{CoCO}$, 178.9°	2072.8(7)	2022.8(6)	2028.6(6)	1.024 72	1.021 79
$\text{Co}(\text{CO})_3$	Co–C, 1.823 Å; C–O, 1.157 Å;	1984.0(1279)	1938.2(1208)	1938.5(1239)	1.023 63	1.023 47
	$\angle\text{CCoC}$, 120°; $\angle\text{CoCO}$, 180°	2060.9(0)	2012.0(0)	2015.8(0)	1.024 30	1.022 37

TABLE 3: Calculated (BP86/6-311+G*) Geometry, Isotopic C–O Stretching Frequencies (cm^{-1}), Intensities (km/mol), and Isotopic Frequency Ratios for $\text{Co}(\text{CO})_x^-$ ($x = 1, 2, 3, 4$) Molecular Anions

anion	geometry	$^{12}\text{C}^{16}\text{O}$	$^{13}\text{C}^{16}\text{O}$	$^{12}\text{C}^{18}\text{O}$	$R(12/13)$	$R(16/18)$
$\text{CoCO}^- ^3\Sigma^+$	Co–C, 1.712 Å; C–O, 1.191 Å; linear	1836.2(912)	1791.0(876)	1798.5(863)	1.025 24	1.020 96
$\text{Co}(\text{CO})_2^- ^1A_1$	Co–C, 1.714 Å; C–O, 1.195 Å;	1783.9(1811)	1740.8(1716)	1746.2(1748)	1.024 76	1.021 59
	$\angle\text{CCoC}$, 125.4°; $\angle\text{CoCO}$, 165.3°	1851.6(559)	1805.5(533)	1814.4(533)	1.025 53	1.020 50
$\text{Co}(\text{CO})_3^-$	Co–C, 1.761 Å; C–O, 1.183 Å;	1830.0(1897)	1786.6(1795)	1790.1(1823)	1.024 29	1.022 35
	$\angle\text{CCoC}$, 120°; $\angle\text{CoCO}$, 180°	1923.1(0)	1876.0(0)	1882.9(0)	1.025 11	1.021 35
$\text{Co}(\text{CO})_4^-$	Co–C, 1.774 Å; C–O, 1.177 Å;	1875.6(1395)	1830.8(1326)	1834.9(1339)	1.024 47	1.022 18
	$\angle\text{CCoC}$, 109.5°; $\angle\text{CoCO}$, 180°	1964.1(0)	1916.5(0)	1922.3(0)	1.024 84	1.021 74

agreement with experiment, the pure DFT functional BP86 was used for subsequent calculations. The dicarbonyl $\text{Co}(\text{CO})_2$ is a bent 2A_1 state with a C–Co–C angle of 171.9°, more open than calculated previously (152°), and the C–O stretching frequencies are about 20 cm^{-1} higher. The tricarbonyl $\text{Co}(\text{CO})_3$ is calculated have a planar D_{3h} symmetry, in agreement with the Swang group.⁸

Calculations were done for $\text{Co}(\text{CO})_{1-4}^-$ anions, and the results are listed in Table 3. The CoCO^- anion was calculated to have a $^3\Sigma^+$ ground state with Co–C and C–O bond lengths 0.03 and 0.021 Å longer than CoCO neutral bond lengths. The $\text{Co}(\text{CO})_2^-$ anion has a 1A_1 ground state with the C_{2v} structure, and the C–Co–C angle is calculated to be 125.4°, more bent than the neutral $\text{Co}(\text{CO})_2$ molecule. The Co–C bond length is 0.085 Å shorter than for the doublet $\text{Co}(\text{CO})_2$ molecule, while the C–O bond is 0.039 Å longer. Both $\text{Co}(\text{CO})_3^-$ and $\text{Co}(\text{CO})_4^-$ have singlet ground states, and the $\text{Co}(\text{CO})_3^-$ anion has D_{3h} symmetry while $\text{Co}(\text{CO})_4^-$ has T_d symmetry.

Discussion

Matrix infrared spectra of cobalt carbonyl complexes and anions will be assigned from isotopic shifts and DFT isotopic frequency calculations.

CoCO. The 1960.7, 1957.3 cm^{-1} bands are assigned to CoCO molecule in two different matrix sites. These bands were observed after deposition in all experiments and decreased on annealing. In $^{13}\text{C}^{16}\text{O}$ and $^{12}\text{C}^{18}\text{O}$ experiments, these bands shifted to 1913.5, 1910.1 and 1920.6, 1917.2 cm^{-1} , respectively. The higher 12/13 ratio (1.0247) and lower 16/18 ratio (1.0209) compared to diatomic CO ratios indicate that the C atom is vibrating between the O atom and another atom. The doublet isotopic structures in both $^{12}\text{C}^{16}\text{O} + ^{13}\text{C}^{16}\text{O}$ and $^{12}\text{C}^{16}\text{O} + ^{12}\text{C}^{18}\text{O}$ experiments confirm that only one CO subunit is involved in this mode. Our DFT calculation predicted the C–O stretching vibration for ground-state CoCO at 1980.5 cm^{-1} , just 20 cm^{-1} higher than the observed value. The calculated isotopic

ratios (12/13, 1.0252) and (16/18, 1.0210) are in excellent agreement with the observed values. This assignment is in reasonable agreement with previous 1956.0 and 1949.0 cm^{-1} observations in an argon matrix.⁶

Co(CO)₂. The 1920.8 cm^{-1} band is assigned to the antisymmetric carbonyl vibration of $\text{Co}(\text{CO})_2$ on the basis of isotopic experiments and DFT calculations. This band was observed after deposition and greatly increased on annealing. It produced 1/2/1 triplets in both mixed $^{12}\text{C}^{16}\text{O} + ^{13}\text{C}^{16}\text{O}$ and $^{12}\text{C}^{16}\text{O} + ^{12}\text{C}^{18}\text{O}$ experiments, indicating that two equivalent CO submolecules are involved. DFT calculation predicted the $\text{Co}(\text{CO})_2$ molecule with near linear structure and strong antisymmetric C–O stretching vibration at 1972.8 cm^{-1} , which is some 52 cm^{-1} too high. The calculated isotopic ratios (12/13, 1.0233; 16/18, 1.0240) are quite close to the experimental ratios (1.0229, 1.0233) and support assignment of the 1920.8 cm^{-1} band to the antisymmetric C–O mode of $\text{Co}(\text{CO})_2$. This observation is in agreement with the previous 1919.0 cm^{-1} assignment to $\text{Co}(\text{CO})_2$ in solid argon.⁶ The symmetric C–O stretching vibration was calculated at 2072.8 cm^{-1} with very low intensity, and this band is not observed here.

Co(CO)₃. The 1983.2 cm^{-1} band appeared on annealing after the $\text{Co}(\text{CO})_2$ absorption. This band produced quartets with two weak intermediate bands in both mixed $^{12}\text{C}^{16}\text{O} + ^{13}\text{C}^{16}\text{O}$ and $^{12}\text{C}^{16}\text{O} + ^{12}\text{C}^{18}\text{O}$ experiments with 12/13 frequency ratio 1.0229 and 16/18 ratio 1.0236, which is suitable for the antisymmetric C–O stretching vibration of the $\text{Co}(\text{CO})_3$ molecule. In previous argon matrix experiments,⁶ a 1982.0 cm^{-1} band was assigned to the $\text{Co}(\text{CO})_3$ molecule, and our result is in excellent agreement. Our DFT calculation predicted the $\text{Co}(\text{CO})_3$ molecule to have D_{3h} symmetry with strong antisymmetric C–O vibration at 1984.1 cm^{-1} , which is just 1 cm^{-1} higher than observed here. In addition the degenerate Co–CO stretching fundamental was calculated at 474.7 cm^{-1} with 12/13 and 16/18 ratios 1.0112 and 1.0193, respectively, which are in excellent agreement with the 463.3 cm^{-1} band and 1.0109 and 1.0187 ratios observed here. This agreement between DFT calculations and matrix infrared spectra confirms the identification of $\text{Co}(\text{CO})_3$.

Co(CO)₄. In previous thermal atom reaction studies,⁶ two bands at 2024.0 and 2014.4 cm^{-1} in solid argon were assigned to a distorted C_{3v} $\text{Co}(\text{CO})_4$ molecule. Similar bands were observed here at 2023.5 and 2016.6 cm^{-1} . These two band appeared on annealing and increased together on further annealing. Recent DFT calculations⁸ concluded that the most stable structure of $\text{Co}(\text{CO})_4$ has C_{3v} symmetry with the D_{2d} structure only 3 kcal/mol higher in energy. The three C–O stretching modes ($2A_1 + E$) were calculated at 2075, 2006, and 1998 cm^{-1} . The 2024.0 and 2014.4 cm^{-1} bands observed in our experiment are just 17.5 and 14.2 cm^{-1} higher than calculations. The other A_1 mode was calculated to have very low intensity and is not observed here. This agreement supports the calculated C_{3v} symmetry of the $\text{Co}(\text{CO})_4$ complex.

CoCO⁻. The sharp band at 1804.0 cm^{-1} observed after deposition decreased on annealing (Figure 2). Filtered photolysis in the 630–1000 nm region decreased, while 470–1000 nm photolysis totally destroyed this band. In $\text{C}^{13}\text{O}^{16}$ and $^{12}\text{C}^{18}\text{O}$ experiments, this band shifted to 1761.0 and 1766.8 cm^{-1} and gave the 12/13 isotopic ratio 1.0244 and 16/18 isotopic ratio 1.0211. In the mixed $^{12}\text{C}^{16}\text{O} + ^{13}\text{C}^{16}\text{O}$ and $^{12}\text{C}^{16}\text{O} + ^{12}\text{C}^{18}\text{O}$ experiments, only pure isotopic counterparts were observed, so only one CO molecule is involved in this vibration. This band is 156.7 cm^{-1} lower than the neutral CoCO molecule absorption, so the CoCO^- anion must be considered analogous to the Fe

and Ni + CO systems, where similar anion absorptions were observed in this region.^{13,14} BP86 calculations predicted the C–O stretching frequency of triplet ground-state CoCO^- at 1836.2 cm^{-1} , some 32.4 cm^{-1} higher than the observed 1804.0 cm^{-1} value, as expected for the DFT calculation. Recall that the same calculation was 20 cm^{-1} high for CoCO . The calculated isotopic ratios (1.0252, 1.0210) are in good agreement with the experimental observations with part of the discrepancy due to the lack of anharmonic correction in the calculations.

The 1807.7 and 1809.2 cm^{-1} bands, also observed after deposition, increased on 20 K annealing and decreased on further annealing. These two bands were destroyed on 470–1000 nm photolysis and exhibited similar isotopic ratios with the 1804.0 cm^{-1} band and doublets in mixed isotopic experiments. These two bands are due to CoCO^- in different matrix environments.

The CoCO^- anions were formed by reaction 1, during the condensation process, which is calculated to be exothermic by 22.3 kcal/mol.



Since the electron affinity of Co is significant (0.66 eV),²³ CoCO^- could be made in these experiments from reaction 3 following the union of laser-ablated Co atoms and electrons.



Since the ablated electrons should be trapped by species other than argon after condensation, the small growth of CoCO^- on annealing is probably due to reaction 2. The electron affinities of FeCO^- and NiCO^- were determined to be 1.26 and 0.8 eV, respectively.^{21,22} In the case of FeCO^- , 630–1000 nm photolysis reduced the band about 20%, but 470–1000 nm radiation destroyed FeCO^- , while for NiCO^- , 850–1000 nm photolysis reduced the NiCO^- absorption about 40%, and 630–1000 nm photolysis destroyed NiCO^- . The matrix photochemistry of CoCO^- is intermediate between FeCO^- and NiCO^- , so one can estimate that the electron affinity of CoCO falls between 0.8 and 1.26 eV. According to calculation, the electron affinity of CoCO is close to 1.0 eV.

The C–O stretching vibration of FeCO^- was observed at 1770.3 cm^{-1} , CoCO^- at 1804.0 cm^{-1} , while the NiCO^- mode was observed at 1847.0 cm^{-1} ; the C–O stretching frequency in these molecular anions increased from Fe to Ni.^{13,14} The same trend was found in the corresponding neutral molecules, FeCO at 1926.0 cm^{-1} , CoCO at 1960.7 cm^{-1} , and NiCO at 1994.4 cm^{-1} , which indicates that the bonding interaction between metal atoms and CO decreases Fe to Ni in both neutral molecules and molecular anions.

Co(CO)₂⁻. The 1768.9 cm^{-1} band observed after deposition increased on lower temperature annealing at the expense of the CoCO^- absorption. This band shifted to 1726.7 and 1732.5 cm^{-1} in $^{13}\text{C}^{16}\text{O}$ and $^{12}\text{C}^{18}\text{O}$ experiments, respectively, and gave the 12/13 ratio 1.0244 and 16/18 ratio 1.0210. In both mixed $^{12}\text{C}^{16}\text{O} + ^{13}\text{C}^{16}\text{O}$ and $^{12}\text{C}^{16}\text{O} + ^{12}\text{C}^{18}\text{O}$ experiments, 1/2/1 triplets were observed, confirming that two equivalent CO molecules are involved. The 1768.9 cm^{-1} band is assigned to the antisymmetric vibration of $\text{Co}(\text{CO})_2^-$. A weak band at 1860.2 cm^{-1} tracked with the 1768.9 cm^{-1} band; the 12/13 ratio 1.0252 was higher than the 1768.9 cm^{-1} band ratio, while the 16/18 ratio 1.0203 was lower than the 1768.9 cm^{-1} band ratio, which is suitable for assignment to the symmetric vibration of a bent $\text{Co}(\text{CO})_2^-$ molecule. The match between the asymmetries of the mixed isotopic triplets confirms these assignments. In the mixed $^{12}\text{C}^{16}\text{O} + ^{13}\text{C}^{16}\text{O}$ experiment, the intermediate component

of the lower triplet was 5.0 cm^{-1} below the mean value of pure isotopic counterparts, while the intermediate component of the upper triplet was 5.1 cm^{-1} higher than the mean value of pure isotopic counterparts.

This assignment is further confirmed by DFT calculations. The BP86 calculation predicted the C–O antisymmetric and symmetric stretching vibrations for the bent singlet ground-state $\text{Co}(\text{CO})_2^-$ at 1783.9 and 1851.6 cm^{-1} , which are in excellent agreement with experimental observations. The calculated 12/13 isotopic ratios 1.0248 (anti), 1.0255 (sym) and 16/18 ratios 1.0216 (anti), 1.0205 (sym) are also a good match to the experimental values listed in Table 1. Finally, the calculated 3:1 infrared intensity ratio is also very close to the observed intensity ratio.

The absorptions of $\text{Co}(\text{CO})_2^-$ increased on annealing at the expense of CoCO^- bands, which suggests reaction 3. This process was also calculated by DFT to be an exothermic reaction. Note that shorter wavelength photolysis is required to bleach $\text{Co}(\text{CO})_2^-$ than CoCO^- .



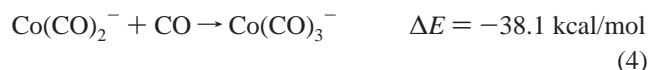
The C–O antisymmetric vibration frequency of $\text{Co}(\text{CO})_2^-$ is lower than the CoCO^- mode; the same relationship is also observed for $\text{Fe}(\text{CO})_2^-$ and $\text{Ni}(\text{CO})_2^-$. The antisymmetric vibration frequency of $\text{Co}(\text{CO})_2^-$ 1768.9 cm^{-1} is lower than those of both $\text{Fe}(\text{CO})_2^-$ and $\text{Ni}(\text{CO})_2^-$, while their neutral molecule modes increased from $\text{Fe}(\text{CO})_2$ to $\text{Ni}(\text{CO})_2$. The ground state of Fe^- is a s^2d^7 quartet,²³ $\text{Fe}(\text{CO})_2^-$ is also a quartet, Ni^- is a s^2d^9 doublet,²² and $\text{Ni}(\text{CO})_2^-$ is also a doublet, so there is no spin change for $\text{Fe}(\text{CO})_2^-$ and $\text{Ni}(\text{CO})_2^-$. In the case of $\text{Co}(\text{CO})_2^-$, the ground state of Co^- is a s^2d^8 triplet,²² but the $\text{Co}(\text{CO})_2^-$ is singlet and a change from triplet to singlet occurs from Co^- to $\text{Co}(\text{CO})_2^-$.

$\text{Co}(\text{CO})_3^-$. The 1826.9 cm^{-1} band appeared only after annealing. Photolysis in the $630\text{--}1000\text{ nm}$ region had no effect, but $470\text{--}1000\text{ nm}$ photolysis decreased the band about 50%, and full arc photolysis destroyed the band. This band shifted to 1784.2 and 1787.6 cm^{-1} in $^{13}\text{C}^{16}\text{O}$ and $^{12}\text{C}^{18}\text{O}$ experiments, respectively, and gave the 12/13 ratio 1.0239 and the 16/18 ratio 1.0220. In both mixed $^{12}\text{C}^{16}\text{O} + ^{13}\text{C}^{16}\text{O}$ and $^{12}\text{C}^{16}\text{O} + ^{12}\text{C}^{18}\text{O}$ experiments, quartets with two weak intermediate bands were produced, indicating that three equivalent CO molecules are involved in this degenerate vibrational mode.²⁴ This band was 136.3 cm^{-1} lower than this mode for neutral $\text{Co}(\text{CO})_3$ molecule, which is appropriate for the $\text{Co}(\text{CO})_3^-$ anion.

The 1820.0 cm^{-1} band was only produced on $470\text{--}1000\text{ nm}$ photolysis, and also destroyed using the full arc. This band exhibited very similar isotopic ratios with the 1826.9 cm^{-1} band. Again, a quartet was produced in the mixed isotopic experiment, which suggests that this band may also due to $\text{Co}(\text{CO})_3^-$ in a different matrix site.

Our DFT calculation predicted $\text{Co}(\text{CO})_3^-$ to have a singlet ground state with planar D_{3h} symmetry, so only one C–O stretching mode is IR active. This was calculated at 1830.0 cm^{-1} , just 3.1 cm^{-1} higher than the major site of $\text{Co}(\text{CO})_3^-$ observed here. The calculated isotopic 12/13 ratio 1.0243 and 16/18 ratio 1.0224 are in very good agreement with the experimental observations.

The $\text{Co}(\text{CO})_3^-$ anions are formed by association reaction 4, which is also highly exothermic.¹²

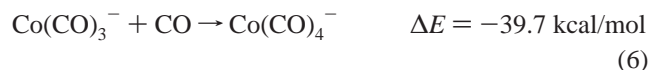


The 1820.0 cm^{-1} matrix site absorption of $\text{Co}(\text{CO})_3^-$ is probably formed by reaction 5 using electrons detached from CoCO^- on 470 nm photolysis.



$\text{Co}(\text{CO})_4^-$. The infrared and Raman spectra of $\text{Co}(\text{CO})_4^-$ have been studied in tetrahydrofuran solution, and a broad band at 1887 cm^{-1} was assigned to the C–O stretching vibration of this molecular anion completely surrounded by solvent.¹¹ A broad 1890.0 cm^{-1} band increased on annealing following $\text{Co}(\text{CO})_3^-$, and it is assigned to $\text{Co}(\text{CO})_4^-$ in solid argon. This band shifted to 1846.3 and 1849.0 cm^{-1} with $^{13}\text{C}^{16}\text{O}$ and $^{13}\text{C}^{18}\text{O}$, respectively, and the isotopic 12/13 ratio 1.0237 is higher while the 16/18 ratio 1.0222 is lower than for the $\text{Co}(\text{CO})_4$ molecule, which suggest more carbon and less oxygen participation in the antisymmetric vibrational mode. This is in accord with the angle change for the $\text{Co}(\text{CO})_3$ subunits in the C_{3v} molecule and the T_d anion. The 1890 cm^{-1} band was destroyed on full arc photolysis, which is consistent with the reported large electron affinity ($\geq 2.35\text{ eV}$).²⁵ In the mixed experiments, the isotopic intermediates cannot be resolved due to isotopic dilution. Our DFT calculations suggest the $\text{Co}(\text{CO})_4^-$ molecular anion to have T_d symmetry with one strong C–O stretching vibration at 1875.6 cm^{-1} , slightly lower than the observed 1890.0 cm^{-1} value in solid argon. The calculated isotopic ratios 1.0245 for 12/13 and 1.0222 for 16/18 are close to the observed values.

The infrared absorption of $\text{Co}(\text{CO})_4^-$ anion was only observed after annealing, indicating that $\text{Co}(\text{CO})_4^-$ is formed by reaction 6, which is exothermic by 39.7 kcal/mol .¹² The $\text{Co}(\text{CO})_4^-$ absorption slightly increased on visible photolysis when CoCO^- and $\text{Co}(\text{CO})_2^-$ were bleached, suggesting that exothermic reaction 7 can also take place.



The elimination of the anion absorptions from the product spectrum with the electron-trapping molecule CCl_4 present in these and earlier $\text{Fe}(\text{CO})_x$ and $\text{Ni}(\text{CO})_x$ experiments^{13,14} adds further support for their anion identification.

Other Absorptions. The weak photosensitive 1515.5 cm^{-1} band for $(\text{CO})_2^-$ is observed here as found in similar Fe and Ni experiments.^{13,14} Several bands at 2053.0 , 2045.5 , and 1862.4 cm^{-1} were produced and increased on annealing and exhibited carbonyl isotopic ratios. In the mixed experiments, the isotopic structure cannot be resolved, and these bands are probably due to $\text{Co}_2(\text{CO})_8$ molecules, on the basis of comparison with earlier work.^{6,26} The broader 2062.4 cm^{-1} band increased strongly on annealing and is clearly due to a higher complex that cannot be identified here. Finally, HCO is detected in several experiments owing to reaction of H atoms from laser dissociation of impurities with CO on the basis of the spectrum reported earlier.²⁷

Conclusions

Laser-ablated cobalt atoms have been reacted with CO molecules during condensation in excess argon. The CoCO molecule is observed after deposition, and $\text{Co}(\text{CO})_{2,3,4}$ are formed on annealing in agreement with earlier matrix work.⁶ Cobalt carbonyl anions are also produced from ablated electrons and trapped in the matrix. On the basis of isotopic substitution and density functional calculations, a sharp absorption at 1804.0

cm^{-1} is assigned to the C–O stretching mode of CoCO^- , 1768.9 and 1860.2 cm^{-1} bands to antisymmetric and symmetric C–O stretching vibrations of bent $\text{Co}(\text{CO})_2^-$, and 1826.9 and 1890.0 cm^{-1} absorptions to the antisymmetric stretching modes of $\text{Co}(\text{CO})_3^-$ and $\text{Co}(\text{CO})_4^-$, respectively. The relative photolysis behavior of FeCO^- , CoCO^- , and NiCO^- suggests an intermediate electron affinity near 1.0 eV for CoCO . The photon energy required to bleach the $\text{Co}(\text{CO})_x^-$ ($x = 1, 2, 3, 4$) molecular anions increases with the number of carbonyls.

Acknowledgment. We thank the National Science Foundation (CHE 97-00116) for financial support.

References and Notes

- (1) Tumas, W.; Gitlin, B.; Rosan, A. M.; Yardley, J. T. *J. Am. Chem. Soc.* **1982**, *104*, 55.
- (2) Keller, H. J.; Wawersik, B. W. *Z. Naturforsch.* **1965**, *206*, 938.
- (3) Fieldhouse, S. A.; Fullam, B. W.; Nielson, G. W.; Symons, M. C. *J. Chem. Soc., Dalton Trans.* **1974**, 567.
- (4) Bidinosti, D. R.; McIntyre, N. S. *Chem. Commun.* **1967**, 1.
- (5) Rest, A. J.; Crichton, O.; Poliakoff, M.; Turner, J. J. *J. Chem. Soc., Dalton Trans.* **1973**, 1321.
- (6) Hanlan, L. A.; Huber, H.; Kundig, E. P.; McGarvey, B. R.; Ozin, G. A. *J. Am. Chem. Soc.* **1975**, *97*, 7054.
- (7) (a) Fournier, R. *J. Chem. Phys.* **1993**, *99*, 1801. (b) Adamo, C.; Leij, F. *J. Chem. Phys.* **1995**, *103*, 10605.
- (8) Ryeng, H.; Gropen, O.; Swang, O. *J. Phys. Chem. A* **1997**, *101*, 8956.
- (9) Burdett, J. K. *J. Chem. Soc., Faraday Trans.* **1974**, *2*, 1599.
- (10) Elian, M.; Hoffmann, R. *Inorg. Chem.* **1785**, *14*, 1058.
- (11) Edgell, W. F.; Lyford, J.; Barbetta, A.; Jose, C. I. *J. Am. Chem. Soc.* **1971**, *93*, 6403.
- (12) Sunderlin, L. S.; Wang, D. N.; Squires, R. R. *J. Am. Chem. Soc.* **1993**, *115*, 12060.
- (13) Zhou, M. F.; Andrews, L. *J. Chem. Phys.*, in press.
- (14) Zhou, M. F.; Andrews, L. *J. Am. Chem. Soc.*, in press.
- (15) Burkholder, T. R.; Andrews, L. *J. Chem. Phys.* **1991**, *95*, 8697. Hassanzadeh, P.; Andrews, L. *J. Phys. Chem.* **1992**, *96*, 9177.
- (16) Thompson, W. E.; Jacox, M. E. *J. Chem. Phys.* **1991**, *95*, 735.
- (17) Frisch, M. J.; Trucks, G. W.; Schlegel, H. B.; Gill, P. M. W.; Johnson, B. G.; Robb, M. A.; Cheeseman, J. R.; Keith, T.; Petersson, G. A.; Montgomery, J. A.; Raghavachari, K.; Al-Laham, M. A.; Zakrzewski, V. G.; Ortiz, J. V.; Foresman, J. B.; Cioslowski, J.; Stefanov, B. B.; Nanayakkara, A.; Challacombe, M.; Peng, C. Y.; Ayala, P. Y.; Chen, W.; Wong, M. W.; Andres, J. L.; Replogle, E. S.; Gomperts, R.; Martin, R. L.; Fox, D. J.; Binkley, J. S.; Defrees, D. J.; Baker, J.; Stewart, J. P.; Head-Gordon, M.; Gonzalez, C.; Pople, J. A. *Gaussian 94, Revision B.1*; Gaussian, Inc.: Pittsburgh, PA, 1995.
- (18) Perdew, J. P. *Phys. Rev. B* **1986**, *33*, 8822. Becke, A. D. *J. Chem. Phys.* **1993**, *98*, 5648.
- (19) McLean, A. D.; Chandler, G. S. *J. Chem. Phys.* **1980**, *72*, 5639. Krishnan, R.; Binkley, J. S.; Seeger, R.; Pople, J. A. *J. Chem. Phys.* **1980**, *72*, 650.
- (20) Wachters, H. J. H. *J. Chem. Phys.* 1970, *52*, 1033. Hay, P. J. *J. Chem. Phys.* **1977**, *66*, 4377.
- (21) Engelking, P. C.; Lineberger, W. C. *J. Am. Chem. Soc.* **1979**, *101*, 5569.
- (22) Stevens, A. E.; Feigerle, C. S.; Lineberger, W. C. *J. Am. Chem. Soc.* **1982**, *104*, 5026.
- (23) Hotop, H.; Lineberger, W. C. *J. Phys. Chem. Ref. Data* **1985**, *14*, 731.
- (24) Darling, J. H.; Ogden, J. S. *J. Chem. Soc., Dalton Trans.* **1972**, 2496.
- (25) Simoes, J. A. M.; Beauchamp, J. L. *Chem. Rev.* **1990**, *90*, 629.
- (26) Blyholder, G.; Allen, M. C. *J. Am. Chem. Soc.* **1969**, *91*, 3158.
- (27) Milligan, D. E.; Jacox, M. E. *J. Chem. Phys.* **1969**, *51*, 277.